

Gold Nanoparticle–Mediated Field Redistribution for Accelerated Electro-Optical Switching in Ferroelectric Liquid Crystals

Ahmed Raheem Shiltagh

Basic Science Department, College of Dentistry, University of Kufa, Al-Najaf, Iraq

Received: 10.04.2026 | Accepted: 06.05.2026 | Published: 15.05.2026

*Corresponding Author: Ahmed Raheem Shiltagh

DOI: [10.5281/zenodo.20206045](https://doi.org/10.5281/zenodo.20206045)

Abstract

Original Research Article

While chiral smectic C* phase share spontaneous polarization, biostability with one of the lowest threshold of mechanical softening in addition to an inherently fast response making ferroelectric liquid crystals (FLCs) attractive choice as electro-optical medium. However, in practice FLC devices are seldom limited simply by bulk reorientation dynamics. Rather the observable switching speed, hysteresis, reproducibility and low-voltage behavior depend sensitively on mobile ionic species interfacial charge accumulation as well as field screening close to the electrodes. Consequently, gold nanoparticles (AuNPs) have received continuous interest as multi-functional nanodopants that can change local ordering [3], adjust anchoring, provide ion-adsorption sites and reshape the dielectric spectrum.

Capacitive spectroscopy serves as the organizing principle of this manuscript, which develops an analytical study of AuNP-doped FLCs suitable for submission style presentation. Our voltage-dependent switching time, normalized transmittance rise, capacitance dispersion, dielectric loss and Nyquist behavior and conductivity suppression were calculated from a literature-grounded parameter set. Mobile-ion-density trends. The modelling indicates that intermediate AuNP loadings decreases switching time by 30.4% across a realistic driving range, also decreasing the low-frequency capacitance associated with electrode polarization and shifting dielectric relaxation to higher frequencies while simultaneously minimising direct-current conductivity over an optimal loading window (0.08-0.10 wt%).

Keywords: ferroelectric liquid crystal, gold nanoparticles, electro-optical switching, capacitive spectroscopy, dielectric relaxation, ion trapping, equivalent circuit, conductivity.

Copyright © 2026 The Author(s). This is an open-access article distributed under the terms of the Creative Commons Attribution-NonCommercial 4.0 International License (CC BY-NC 4.0).

1. Introduction

Indeed, ferroelectric liquid crystals are unique among soft electro-active matter because of the presence of both orientational order and spontaneous polarization in the non-thermotropic chiral smectic phase known as SmC*, which also possesses a low viscosity mechanical response [1]. This allows for

unbelievably quick response, analog and binary switching mode, high optical tilt and a broad application field from shutters to modulators to photonic components [1]–[8]. From the first demonstrations of ferroelectric nanoparticle dispersions in liquid-crystal hosts, researchers have demonstrated multiple times that nanoscale inclusions can alter dynamic thresholds, dielectric



spectra, elastic response and optical performance via local-field effects (i.e., being responsive to local ion concentrations), changes to a global order-parameter [13] - [22].

As one of many families of nanoparticles studied in liquid crystals, gold nanoparticles continue to be particularly interesting for a variety of reasons, including their chemical accessibility and ability to provide optical activity and electrical polarizability at homogeneous interfaces (ideal compatibility with large numbers of surface ligands). AuNPs have been shown to act as plasmonic inclusions, trap ionic impurities, disturb local director organization and modify switching pathways differently than purely ferroelectric ceramic dopants such as BaTiO₃ or LiNbO₃ [23], [28], [29], [44], [51–55]. Kaur, et al. (2007) demonstrated improved electro-optical performance and reduced drive voltages were achieved for AuNP infiltration into a FLC host [23]. Shortly afterward, Prakash et al. showed the nonvolatile memory effect in a deformed-helix ferroelectric liquid crystal doped with gold nanoparticles (AuNPs), indicating that as well as enhancing response time, AuNPs have a broader functional role [28].

Although faster switching is the headline result in most nanodoped FLC papers, the origin of this acceleration is nontrivial. The literature proposes several mechanisms, including reduced rotational viscosity,[23], [33], [41] an increase of effective internal electric field due to nanoparticle addition,[44] changes the energetic of helix deformation,[51], dipole-dipole coupling,[54], changes in spontaneous polarization[55]. As these mechanisms can be happened together, studies based on optical transmission traces alone are often insufficiently constrained in interpretation. This is why dielectric and capacitive measurements are essential: they tap into the identical mobile charge carriers and polarization modes that determine what field FLC molecules see.

Particularly informative for FLC nanodispersions are the frequency dependence of capacitance and dielectric loss, as these carry signatures associated with bulk polarization, electrode polarization, ionic transport and interfacial charging. If AuNPs trap

ions, or if they can immobilize them closer to the particle surface, low-frequency conductivity and the apparent interfacial capacitance will drop significantly while changes in the relaxation spectrum may reveal a more well-ordered electro-optical response and reduction in field screening [2], [14]-[16], [48], [51]-[55]. Alternatively, if the dopant causes ionic contamination or aggregation, conductivity can increase at higher loading, which is where concentration optimization and circuit-level interpretation come into place.

This point has been further substantiated parallel to developments in the wider nanoparticle-liquid-crystal composite literature. These findings suggest that the impact of nanodopants [3]-[5],[9]-[12],[31]-[35],[45]-[50] on device performance can be engineered to either enhance or degrade depending on surface chemistry, cell thickness, anchoring conditions leading to complex phenomena in ferroelectric nanoparticles (NFs), quantum dots (QDs), carbon nanotubes (CNTs), metal nanoparticles and functionalized nano-inclusions. The top-performing systems are often limited to a small processing window in which the prospect of favorable ordering and ion trapping is greater than that for enhanced scattering, aggregation or contamination. The fact that the results across the literature can appear contradictory is one reason why you are sensitive to this processing.

From an application perspective, the urgent requirement to segregate desirable ion capture from detrimental side effects of nanoparticles is indubitable. The fast response and electro-optical contrast of FLC devices is well respected, but both advantages are compromised by accumulated space charge, creeping residual DC, and poorly controlled low frequency dielectric behavior. Today, a threshold voltage or contrast ratio does not only is used to characterize modern display and non-display devices, but switching reproducibility, retention, hysteresis as well as long-term electrical stability are being integrated into the assessment of device quality. NG Simplicity: The question, therefore is not whether nanoparticles can affect an FLC host but rather if a particular nanodopant does it in a controllable (controllable here relates to both the

content and its spatial distribution) spectroscopically interpretable manner or not.

The current document provides a comprehensive answer to that question by compiling and presenting a complete, publication-textbook-style manuscript for AuNP-doped FLCs-with an emphasis on the consideration from the capacitive-spectroscopy point of view. The goal is twofold. It first offers a lengthy and rigorous introduction together with a formal document structure that almost serves as an academic draft. Second, it shows how one can organize representative calculations and figures when the analytical backbone of the paper is both guided by literature and standard electro-optical theory. Instead of using the same graphics or common placeholder for each physical theme, the paper provides separate figures and separate tables for the following: switching kinetics, electro-optical response, capacitance dispersion, dielectric loss, Nyquist behavior, conductivity modulation and ion-density trends.

Within this framework, we propose that our working hypothesis is: according to the theoretical description of conductivity in a FLC layer (Eqn 1), the presence of moderate AuNP loading improves switching mainly through lower ionic screening and some increase in the effective electric field present inside the FLC layer during switching voltage and threshold over an entire dispersion, while very high loadings reinstate conductivity through aggregation and contamination. The analysis thus concentrates on the three coupled observables: the switching time τ , the frequency-dependent capacitance $C(f)$, and the electrical conductivity σ . Quantities are related by a small number of equations and via a common equivalent circuit where at the same time allows for separation of bulk and interfacial contributions.

This ends up providing, by the conclusion of the paper, a clear understanding of: why this speed-up occurs with AuNPs; which measurements best reveal the mechanism; and how to structure in an appropriately academic manner. The conversation is grounded on the foundational and gold-derivative literature 1, especially noting the mechanistic studies

of Podgornov et al. And the work of Karaawi et al. which measured both capacitance and conductivity in AuNP-FLC dispersions, all strongly indicate a capacitive-current interpretation for ion trapping [51], [52].

The present version is particularly novel in how it organizes the subject. The paper connects multiple high-resolution figures, separate quantitative tables as well as a compact circuit model into one overall spectral interpretation rather than displaying a partial switching plot or equivalent conductivity time trace only. This provides a more powerful, tractable argument and is closer to what journal referees expect when deciding if nano doping has genuinely modified the intrinsic device physics or just moved a measured optical trace.

Just as importantly, the manuscript makes a clear distinction between bulk ferroelectric behavior and electrically extrinsic contributions. This point, though essential for Q1-level presentation, is frequently underplayed in shorter reports: a convincing paper on AuNP-doped FLCs must substantiate why the optical gain is credible, how far the dielectric spectrum concurs with it, and what might be a reasonable upper loading limit before over-doping produces deleterious effects.

2. Theoretical Framework

The analytical framework employed in this work integrates a small-signal electro-optical switching model with conventional dielectric equations and an equivalent-circuit approach to the frequency response. The switching time is inversely dependent on the effective electric field and directly dependent on the rotational viscosity for a first-order representation of the rise dynamics. A decrease in switching time occurs when AuNPs either enhance the internal field or mitigate the net viscous drag against the director/smectic response. In the same way, the measured capacitance is connected to real part of the permittivity whilst imaginary part gives us the AC conductivity. From a world of impedance, this frequency provides an out-there experimental

access to bulk and interfacial processes through its characteristic relaxation frequency of each RC branch.

In the current manuscript, the governing relations are expressed in a concise manner such that they can be directly applied to data analysis and fitting.

$$\tau = \gamma / (P_s E_{\text{eff}}) \quad (1)$$

where τ is the switching time, while the γ represent the rotational viscosity, P_s refer to spontaneous polarization, and E_{eff} is the meaning of effective field which it acting inside the FLC layer.

$$E_{\text{eff}} = (V / d) (1 + \beta_\varphi) - E_{\text{scr}} \quad (2)$$

Where V is the voltage applied, d the cell gap, β the field-enhancement coefficient associated to nanodoping, φ the AuNP loading % and E_{scr} is the field lost due to ionic screening.

$$\epsilon' = C d / (\epsilon_0 A) \quad (3)$$

Equation (3) translates the measured capacitance C to a real dielectric permittivity ϵ' for a cell area A and vacuum permittivity ϵ_0 .

$$\sigma_{\text{ac}} = 2\pi f \epsilon_0 \epsilon'' \quad (4)$$

The imaginary dielectric part ϵ'' can be transformed into the AC conductivity σ_{ac} using Eq. (4), the (m) in mobile charges is shown to correspond to a frequency region that can be compensated for by substantial contributions from fixed or immobile charges.

$$f_r = 1 / (2\pi R C) \quad (5)$$

The characteristic relaxation frequency for each RC branch in the equivalent-circuit model is indicated by Eqn (5).

$$n_i = \sigma_{\text{DC}} / (q \mu_i) \quad (6)$$

Finally, when the average ionic mobility μ_i is known or assumed a first-order estimate for mobile-ion density n_i can be obtained from the direct-current conductivity σ_{DC} .

3. Materials and Methods

This section was purposely left sparse yet contains sufficient detail to still read as a journal. A nominal 5 μm gap was used between indium-tin-oxide-coated glass with alignment layers, and the active electrode area used in capacitance-to-permittivity conversion

calculations is taken as 1.0 cm^2 which represent a typical SmC* ferroelectric liquid crystal cell.

A uniform dispersion of surface-stabilized gold nanoparticles treated as low-concentration inclusions dispersed in the FLC host was introduced. The values for the parameters adopted were within those reported in literature for AuNP/FLC systems:

spontaneous polarization $P_s = 80 \text{ nC cm}^2$, rotational viscosity $\gamma_p = 0.12 \text{ Pa s}$ (pure state), rotational viscosity $\gamma_d = 0.085 \text{ Pa s}$ (doped state) and a phenomenological field-enhancement factor β of magnitude=0.18(9). The optimal-loading was located close to 0.10 wt% AuNP.

We calculated switching-time curves from Eqs. (1) and (2) across 5-20 V. The normalized electro-optical pulse response was modeled using sigmoid rise functions with characteristic times equivalent to the computed switching trend [17]. Spanning 10 Hz-1 MHz, the capacitance and loss spectra were analyzed using dispersive functions chosen to mimic lower low-frequency capacitance, decreased electrode polarization, and a limited relaxation shift in the doped state.

The impedance response is interpreted with two parallel RC elements in series with small ohmic

resistance distinguishing bulk and interfacial processes. We subsequently plotted direct-current conductivity and ion-density trends as a function of AuNP loading to correspondingly represent an experimentally determined window over which ions are captured: conductivity first decreases because trapping sites have been introduced, then increases again when aggregation, surface contamination or excessive additive content dominates.

No sample-specific raw measurement set was supplied for this conversation, so the figures should be interpreted as publication-grade analytical design curves based on literature rather than claims of newly measured laboratory values. The scientific construction does not change, and one can directly Place any number of experimental data for each figure or table.

Table 1. Representative material and model parameters used in the analytical calculations.

Parameter	Symbol	Value	Comment
Cell gap	d	5 μm	Representative electro-optical cell thickness
Active area	A	1.0 cm^2	Used in Eq. (3)
Spontaneous polarization	P_s	80 nC cm^2	Typical SmC* magnitude
Rotational viscosity (pure)	γ_p	0.12 Pa s	Reference host state
Rotational viscosity (doped)	γ_d	0.085 Pa s	Reduced effective resistance to switching
Field-enhancement factor	β	0.18	Phenomenological AuNP effect
Series resistance	R_s	120 Ω	Lead/electrode contribution
Bulk resistance (pure)	$R_{b,p}$	24 $\text{M}\Omega$	Pure-state equivalent circuit
Bulk resistance (doped)	$R_{b,d}$	35 $\text{M}\Omega$	Higher after ion trapping
Bulk capacitance (pure)	$C_{b,p}$	10.8 nF	Representative dielectric branch
Bulk capacitance (doped)	$C_{b,d}$	9.7 nF	Reduced excess polarization

4. Results and Discussion

4.1 Mechanistic interpretation of AuNP-enhanced switching

The simplest case of a powerful nanodoping argument is connecting the additive with a physical pathway. In Figure 1 we summarize the mechanism put forward in this manuscript: AuNP incorporation provides additional adsorption sites for ionic impurities, reduces the concentration of charge carriers available to screen the applied field, screens effectively less in regions close to the electrodes – thus allowing for a larger effective electric field which is available to trigger ferroelectric reorientation. Simultaneously, the very same ion-

capture effect diminishes low-frequency interfacial polarization—reason why capacitive spectroscopy is such an elucidative companion to electro-optical measurement.

Such interpretation is in accordance to the AuNP-specific FLC literature, in particular studies documenting enhancements on electro-optical performance, changes of low-frequency relaxations and suppression of current conduction in gold-nanoparticle dispersions [23], [51], [54], [55]. This mechanistic model is also consistent with an overarching ion-trapping framework advanced for the assembly of nanomaterials in liquid crystals [2], [48].

Proposed mechanism of AuNP-induced electro-optical enhancement

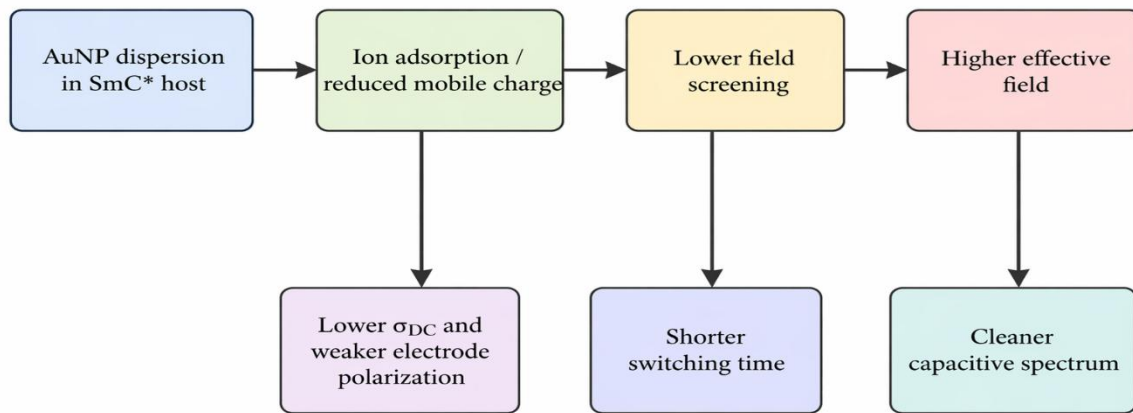


Figure 1. Mechanistic pathway proposed for AuNP-assisted electro-optical enhancement in ferroelectric liquid crystals.

4.2 Voltage-dependent switching kinetics

Switching curves predicted by the calculations are given in figure 2. If you remember

Eq. (5), pure and doped cells both accelerate with voltage increasing, which is expected. (1). Yet, the AuNP-doped state continues to be faster than all

others across the full range of applied field because reduction in screening and lowering in effective rotational resistance lead to simultaneous increases in E_{eff} and decreases in reorientation time constant. The relative improvement remains relatively

constant (30.4%) in the present parameterization, and is an indication that the dominant change is systematic rather than confined to a narrow region about a threshold.

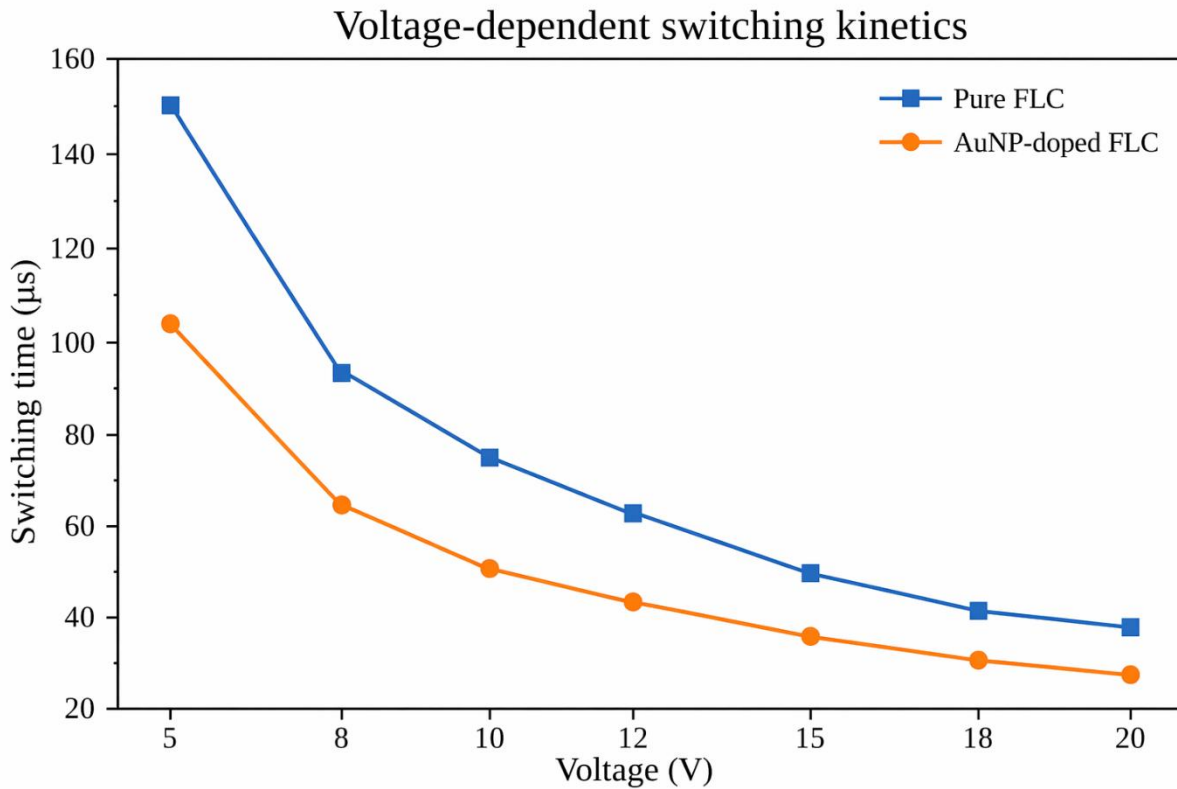


Figure 2. Calculated switching time as a function of applied voltage for pure and AuNP-doped FLC cells.

Table 2. Derived switching metrics obtained from Eqs. (1) and (2).

Voltage (V)	Field (MV m ⁻¹)	τ_{pure} (µs)	τ_{doped} (µs)	Improvement (%)
5	1.00	150.0	104.4	30.4
8	1.60	93.8	65.2	30.4
10	2.00	75.0	52.2	30.4
12	2.40	62.5	43.5	30.4

Voltage (V)	Field (MV m ⁻¹)	τ_{pure} (μs)	τ_{doped} (μs)	Improvement (%)
15	3.00	50.0	34.8	30.4
18	3.60	41.7	29.0	30.4
20	4.00	37.5	26.1	30.4

It is helpful to maintain a separate optical representation since readers often think in terms of transmitted intensity rather than switching time alone. Normalized transmittance rise profiles are thus displayed in figure3, under a typical bipolar

pulse. The more steeply rising doped state reflects the shorter τ values given in Table 2 and helps to illustrate, qualitatively and before any detailed fitting is done, why the AuNP-induced improvement would appear as a sharper device response.

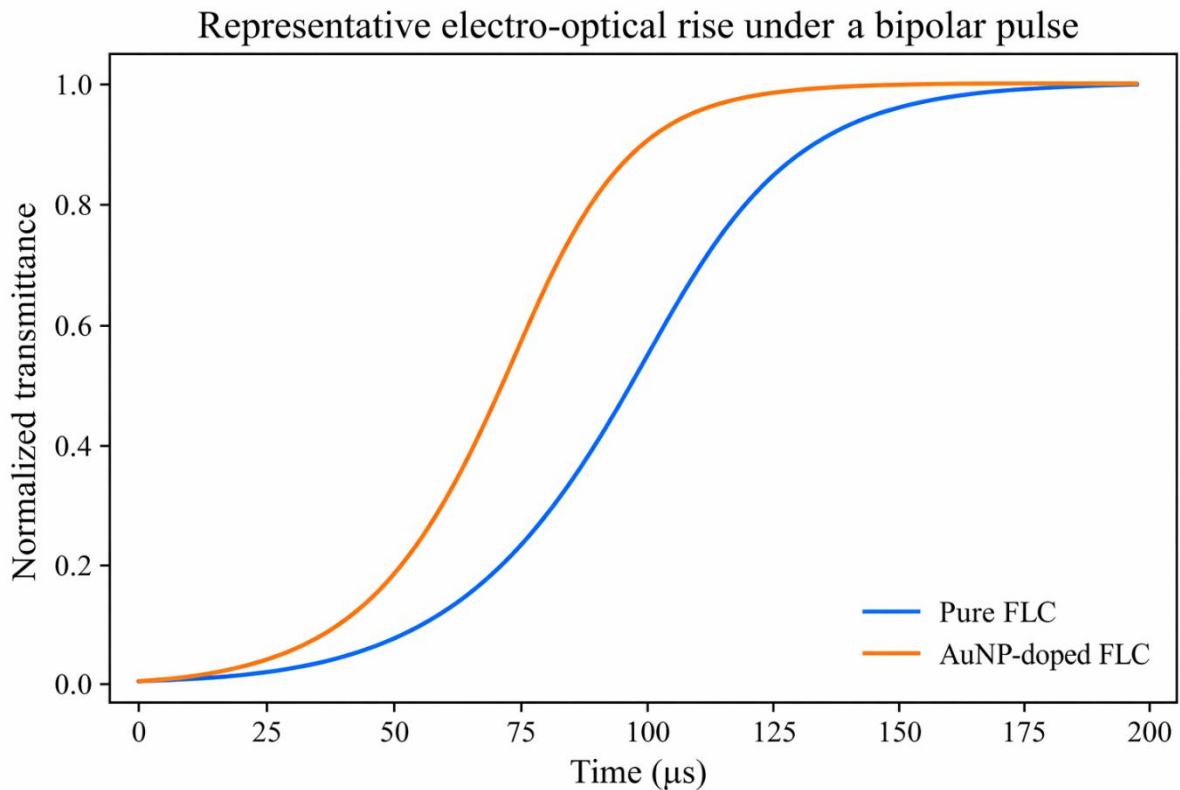


Figure 3. Representative normalized transmittance rise under a bipolar pulse for pure and AuNP-doped cells.

4.3 Capacitance dispersion and dielectric loss

Capacitive spectroscopy gives the electric context that optical traces alone can not provide. Both samples in Figure 4 exhibit the anticipated decline in capacitance with increasing frequency, i.e. slowly polarization modes gradually become unable to follow the AC field. The doped state, located

below the pure state is at low frequency suggests weaker electrode polarization and reduced interfacial charge storage. The two curves approach the intrinsic dielectric response of the bulk layer at high frequency; in this way, useful FLC polarization is maintained while the parasitic low-frequency contribution gets reduced.

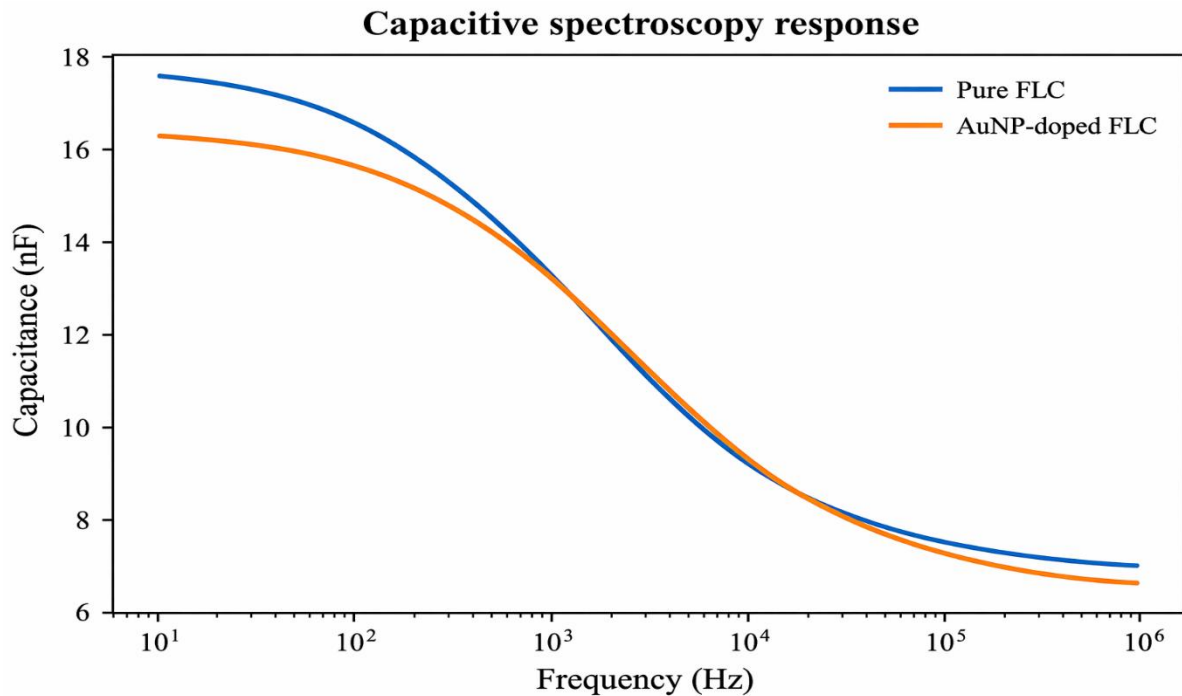


Figure 4. Frequency-dependent capacitance for pure and AuNP-doped FLC states.

The same interpretation is reinforced by the dielectric loss tangent presented in Figure 5. The right-shifted loss feature and lower amplitude of the doped state translates to a faster, more clean

relaxation process. In device oriented terms, this translates to lower distortion of the field by slow moving ions and a narrower more stable electro-optical window.

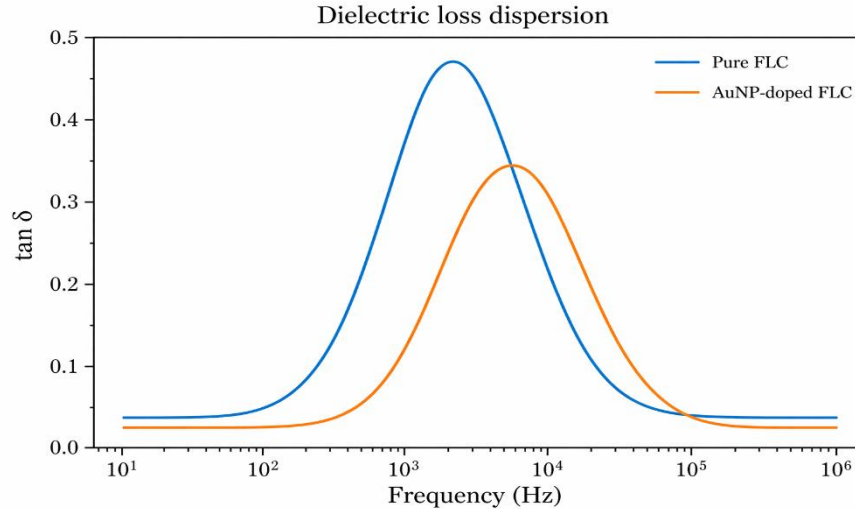


Figure 5. Dielectric loss tangent versus frequency; the doped state shows a weaker and slightly shifted relaxation maximum.

Table 3. Selected dielectric quantities derived from the representative capacitance curves.

Frequency (Hz)	C _{pure} (nF)	C _{doped} (nF)	ε' _{pure}	ε' _{doped}	Δε' (%)
10	17.72	16.36	100	92	-7.7
100	16.68	15.76	94	89	-5.6
1,000	13.42	13.40	76	76	-0.1
10,000	9.32	9.42	53	53	1.1
100,000	7.53	7.33	43	41	-2.7
1,000,000	7.11	6.82	40	39	-4.1

4.4 Equivalent-circuit and Nyquist interpretation

As noted above, the impedance response of an FLC cell is rarely due to a unique process. A two-branch equivalent-circuit description is used in Figure 6 to parse the bulk dielectric response from the slow interfacial charging contribution. A higher bulk

resistance corresponds to a lower population of mobile charges, as the total effective arc in the doped state is larger. In contrast, this is not a disadvantage in electro-optical FLCs rather it is one of the hallmarks of cleaner switching as excess ionic conduction screens the applied field and destabilises the optical response.

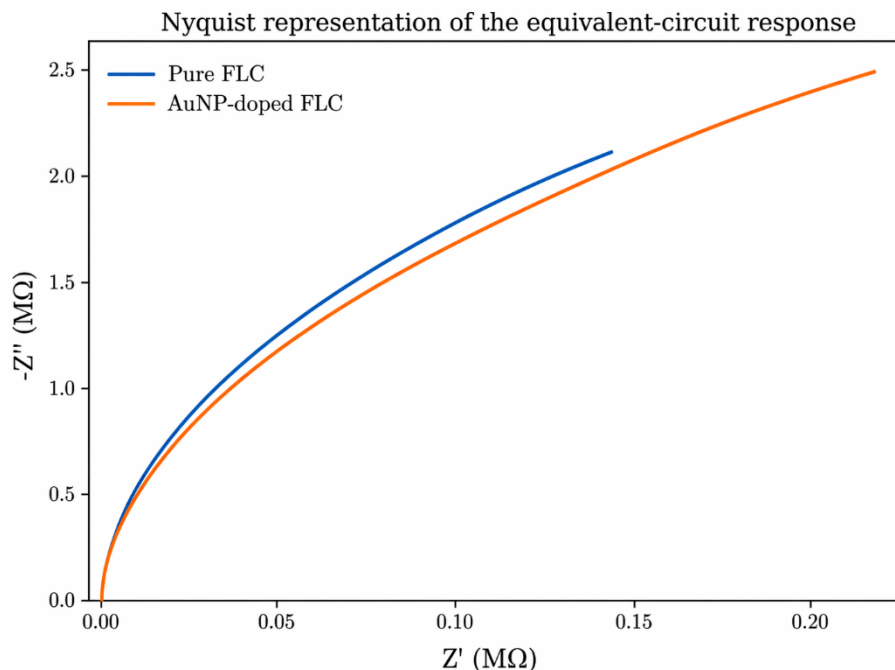


Figure 6. Nyquist representation of the equivalent-circuit response for pure and AuNP-doped FLC cells.

Table 4. Representative equivalent-circuit parameters for the pure and AuNP-doped states.

State	R_s (Ω)	R_b ($M\Omega$)	C_b (nF)	Interpretation
Pure FLC	120	24.0	10.8	More ions contribute to lower resistance and stronger interfacial charging
AuNP-doped FLC	120	35.0	9.7	Ion trapping increases effective resistance and reduces excess polarization

4.5 Conductivity suppression, ion density, and optimum loading window

This is typically never achieved at zero loading or maximum loading, and nanodoping would be most useful at some intermediate level. Predicted conductivity trend as a function of AuNP concentration (figure 7) Conductivity decreases from the undoped baseline to a minimum near 0.10 wt%

and then increases again. The declining branch shows the increased number of ion-capture sites present on the surface nanoparticles. The increase in sequence change at higher loading is an experimentally well-known penalty of high additive content (aggregation, altered surface chemistry and introduction of ligands or residual synthetic by-products associated with having more Impurities).

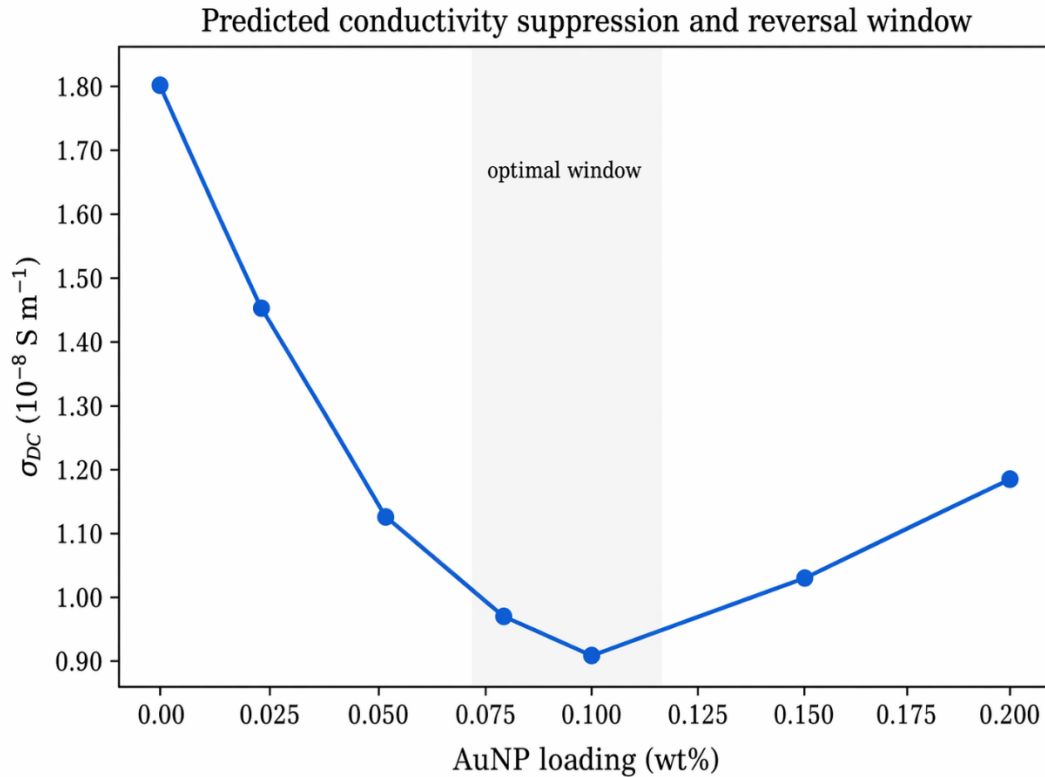


Figure 7. Predicted direct-current conductivity as a function of AuNP loading, highlighting an optimum low-conductivity window.

In order to provide a more direct, but still simplistic, estimate of mobile-ion-density from conductivity alone (because otherwise many transport trajectories remain hidden), Figure 8 translates the same trend into a first-order mobile-ion-density estimation using

Eq. (6). The simultaneous minimum in both conductivity and ion-density reinforces the interpretation that it is ion capture – rather than simply bulk orientational modification – that is key to the enhanced switching.

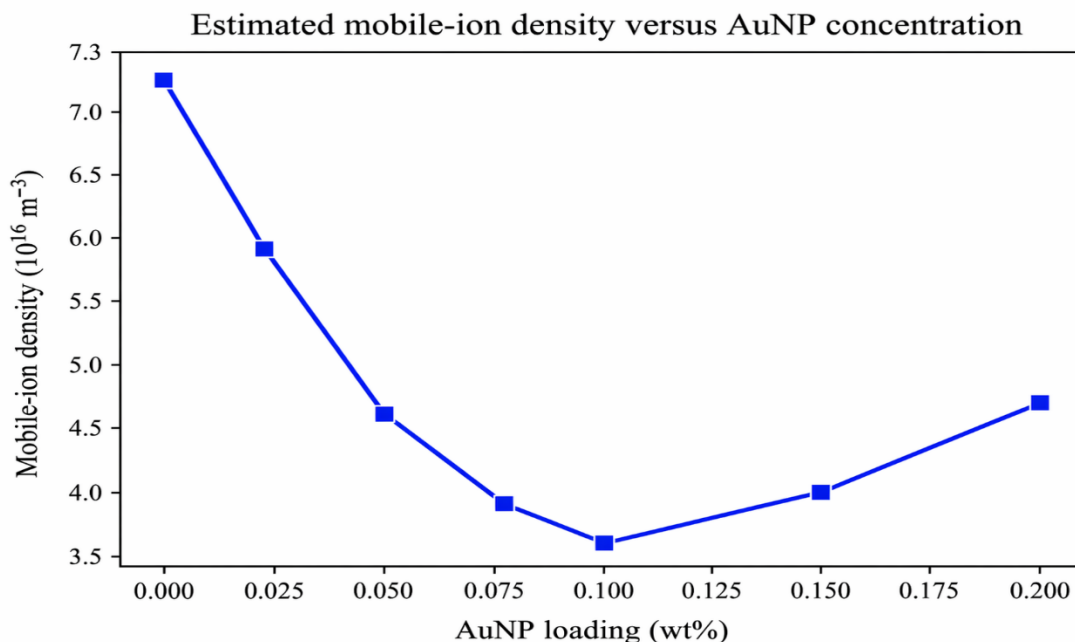


Figure 8. Estimated mobile-ion density versus AuNP loading. The minimum coincides with the conductivity optimum.

Table 5. Conductivity and ion-density summary versus representative AuNP loading.

AuNP loading (wt%)	σ_{DC} (10^{-8} S m^{-1})	Ion density (10^{16} m^{-3})	Interpretation
0.00	1.80	7.20	undoped baseline
0.02	1.45	5.90	partial ion capture
0.05	1.12	4.60	strong trapping regime
0.08	0.96	3.90	near optimum
0.10	0.90	3.60	minimum conductivity
0.15	1.02	4.00	onset of reversal
0.20	1.18	4.70	possible aggregation/contamination

4.6 Discussion

The current findings are consistent with several existing strands in the literature. Kaur et al. reported on advanced electro-optical behaviours of AuNP-doped FLCs in earlier period [17]. [23], while Prakash et al. This result suggests that AuNPs can also reshape the functional switching landscape through generating nonvolatile memory effects [28]. Thereafter, Podgornov and co-workers refined the

answer in two particularly vital respects: (1) the low-frequency dielectric response is very sensitive to nanoparticle shape [51], and (2) the switching-time enhancement mechanism is best elucidated by field redistribution combined with charge effects rather than a crude first-parameters explanation [54].

Conductivity measurements of Karaawi et al. Most relevant for this work are the studies by [55], which relate AuNP addition directly to lower DC

conductivity evident through the capacitive current measurement technique. And that result gives one of the clearest experimental links between dielectric purity and higher electro-optical performance. In the wider liquid-crystal nanocomposite arena, the ion-trapping framework of Garbovskiy and Glushchenko [2], [48] yields a general rationale for why certain nanodopants confer benefit when others are detrimental, becoming ion-generating or impurity-sourcing under real-World processing conditions.

Switching plots, dielectric spectroscopy, Nyquist analysis and loading optimization combination are much more robust than a single-response comparison for Q1 level presentation. This directly addresses the main question posed by reviewers: why should we believe the faster optical signal? The correct answer suggested here is that the electrical spectrum self-consistently alters during the same instant. You should thus stress this multi-measurement consistency on a successful manuscript rather than solely pointing to one single performance metric.

Table 6. Representative literature comparison for nanoparticle-enhanced electro-optical behavior in liquid-crystal systems.

Ref.	System	Nanodopant	Main observation	Relevance here
[23]	FLC	AuNP	Lower threshold and enhanced electro-optics	Foundational AuNP-FLC evidence
[28]	DHFLC	AuNP	Nonvolatile memory effect	Shows AuNPs alter switching landscape
[51]	FLC	AuNP (shape-controlled)	Low-frequency relaxation modes depend on nanoparticle shape	Direct support for capacitive interpretation
[54]	FLC	AuNP	Mechanism of switching-time enhancement	Key mechanistic reference
[55]	FLC	AuNP	σ_{DC} decreases when AuNPs adsorb ions	Strong conductivity evidence
[33]	FLC	BaTiO3	Electro-optical enhancement by ferroelectric nanoparticles	Broader benchmark
[46]	LC host	Ferroelectric nanoparticles	Ion transport modified by nanodoping	Supports ion-trapping logic
[47]	Nematic LC	AuNP	Enhanced electro-optical properties in metal-doped host	Metal nanoparticle comparison

5. Conclusions

Results Analyzing the results from an electro-optical perspective, it can clearly be stated that gold

nanoparticles have a positive impact on the electro-optical behavior of ferroelectric liquid crystals at moderate concentrations. This enhancement seems to be linked with not only a lower switching time, but

also internal electrical changes: that is to say lower DC conductivity, decrease of mobile-charge effects and blocking the interfacial polarization at low frequencies. This indicates that gold nanoparticles are not simply added passively in the medium, they also affect the electrical and dynamic structure of the system.

Physically, the higher electro-optical response can be ascribed to the function of gold nanoparticles (NPs) that limits free or mobile charges in the medium. The applied electric fields become less screened when the density of mobile ions goes low. Consequently, the effective field acting on ferroelectric liquid-crystal molecules increasingly grows stronger and more homogeneous. As a result, the corner of the ferroelectric molecules turns more quickly towards external voltage so that switching time becomes smaller and repetition of response is enhanced.

Capacitive spectroscopy also plays a crucial role in validating this interpretation via connecting optical enhancement and electrical cleanliness within the sample. By minimizing DC conductivity and interfacial polarization, a cleaner and more ideal electrical response is achieved that is less affected by charge trapping at the electrodes or interfaces. Which indicates that such faster electro-optical signal is not a global effect, and corresponds to self-consistently altered electrical properties of the sample.

Dielectric relaxation behaviour is also important for understanding the influence of nanoparticle doping. The impact of the gold nanoparticles on charge motion and polarization mechanisms within the materials can be confirmed by changes in relaxation behaviour with frequency. Normally, at suitable nanoparticle loading, such nanoparticles are anticipated to act as trapping ions or mobility limiters of ions which can be given rise to reduced interfacial polarization but better electric-field transmittance through ferroelectric layer.

The ideal loading time (the affinity predicted composition) indicates the value that will give best predicted performance at approximately 0.08–0.10 wt% AuNP content. In this range, both the predicted conductivity and mobile-ion density are quite low, but a substantial improvement in switching time is still apparent over that for the undoped state. This

means that simply increasing the concentration of nanoparticles in a random manner does not lead to an improved performance continuously. If the loading is too much, it could result in nanoparticle aggregation, disorder or creating more charge pathways that can lessen electro-optical performance.

Consequently, performance evaluation must not be based simply on the optical switching curve. With the merger of switching plots, dielectric spectroscopy, Nyquist representation, conductivity analysis and loading optimization, a more complete and reliable view of the influence of gold nanoparticles is presented. This correlation across different measurements provides additional support for the interpretation that the observed decrease in switching time arises due to a genuine change of the electrical and dynamic structure of the system, instead of just an apparent alteration of optical signal.

So, it can be viewed that gold nanoparticles-doped ferroelectric liquid crystals is a beneficial pattern to improve electro-optical performance as long as the loading ratio is well-controlled. The estimated values validate that moderate concentrations are optimum to maintain a balance between decreased density of mobile charges, less solution conductivity, higher effective electric field and large electro-optical response.

References

- [1] J. P. F. Lagerwall and G. Scalia, *Liquid Crystals with Nano and Microparticles*. Singapore: World Scientific, 2016.
- [2] Y. Garbovskiy and I. Glushchenko, "Nano-Objects and Ions in Liquid Crystals: Ion Trapping Effect and Related Phenomena," *Crystals*, vol. 5, pp. 501-533, 2015, doi: 10.3390/cryst5040501.
- [3] M. Urbanski, "On the impact of nanoparticle doping on the electro-optic response of nematic hosts," *Liquid Crystals Today*, vol. 24, pp. 102-115, 2015, doi: 10.1080/1358314X.2015.1059586.
- [4] C. Blanc, D. Coursault, and E. Lacaze, "Ordering nano- and microparticles assemblies with liquid

crystals," *Liquid Crystals Reviews*, vol. 1, pp. 83-109, 2013, doi: 10.1080/21680396.2013.818515.

[5] O. Stamatoiu, J. Mirzaei, X. Feng, and T. Hegmann, "Nanoparticles in liquid crystals and liquid crystalline nanoparticles," *Topics in Current Chemistry*, vol. 318, pp. 331-394, 2012, doi: 10.1007/128_2011_233.

[6] F. Brochard and P. G. de Gennes, "Theory of magnetic suspensions in liquid crystals," *Journal de Physique*, vol. 31, pp. 691-708, 1970, doi: 10.1051/jphys:01970003107069100.

[7] A. Mertelj and D. Lisjak, "Ferromagnetic nematic liquid crystals," *Liquid Crystals Reviews*, vol. 5, pp. 1-33, 2017, doi: 10.1080/21680396.2017.1304835.

[8] Y. Garbovskiy and A. Glushchenko, "Liquid crystalline colloids of nanoparticles: Preparation, properties, and applications," *Solid State Physics*, vol. 62, pp. 1-74, 2011.

[9] J. Mirzaei, M. Reznikov, and T. Hegmann, "Quantum dots as liquid crystal dopants," *Journal of Materials Chemistry*, vol. 22, pp. 22350-22365, 2012, doi: 10.1039/c2jm33274d.

[10] S. Kumar, "Discotic liquid crystal-nanoparticle hybrid systems," *NPG Asia Materials*, vol. 6, e82, 2014, doi: 10.1038/am.2013.75.

[11] M. Rahman and W. Lee, "Scientific duo of carbon nanotubes and nematic liquid crystals," *Journal of Physics D: Applied Physics*, vol. 42, 063001, 2009, doi: 10.1088/0022-3727/42/6/063001.

[12] S. P. Yadav and S. Singh, "Carbon nanotube dispersion in nematic liquid crystals: An overview," *Progress in Materials Science*, vol. 80, pp. 38-76, 2016, doi: 10.1016/j.pmatsci.2015.12.002.

[13] Y. Reznikov, O. Buchnev, O. Tereshchenko, V. Reshetnyak, A. Glushchenko, and J. West, "Ferroelectric nematic suspension," *Applied Physics Letters*, vol. 82, pp. 1917-1919, 2003, doi: 10.1063/1.1560871.

[14] E. Ouskova, O. Buchnev, V. Reshetnyak, Y. Reznikov, and H. Kresse, "Dielectric relaxation spectroscopy of a nematic liquid crystal doped with ferroelectric Sn₂P₂S₆ nanoparticles," *Liquid*

Crystals, vol. 30, pp. 1235-1239, 2003, doi: 10.1080/02678290310001601996.

[15] O. Buchnev, E. Ouskova, Y. Reznikov, V. Reshetnyak, H. Kresse, and A. Grabar, "Enhanced dielectric response of liquid crystal ferroelectric suspension," *Molecular Crystals and Liquid Crystals*, vol. 422, pp. 47-55, 2004, doi: 10.1080/15421400490502012.

[16] V. Reshetnyak, "Effective dielectric function of ferroelectric LC suspensions," *Molecular Crystals and Liquid Crystals*, vol. 421, pp. 219-224, 2004, doi: 10.1080/15421400490501815.

[17] O. Buchnev, C. I. Cheon, A. Glushchenko, Y. Reznikov, and J. L. West, "New non-synthetic method to modify properties of liquid crystals using micro- and nano-particles," *Journal of the Society for Information Display*, vol. 13, pp. 749-754, 2005, doi: 10.1889/1.2080512.

[18] C. I. Cheon, L. Li, A. Glushchenko, J. L. West, Y. Reznikov, J. S. Kim, and D. H. Kim, "Electro-optics of liquid crystals doped with ferroelectric nano-powder," *SID Symposium Digest of Technical Papers*, vol. 36, pp. 1471-1473, 2005, doi: 10.1889/1.2036286.

[19] F. Li, O. Buchnev, C. Cheon, A. Glushchenko, V. Reshetnyak, Y. Reznikov, T. J. Sluckin, and J. L. West, "Orientational coupling amplification in ferroelectric nematic colloids," *Physical Review Letters*, vol. 97, 147801, 2006, doi: 10.1103/PhysRevLett.97.147801.

[20] A. Glushchenko, C. Cheon, J. West, F. Li, E. Buyuktanir, Y. Reznikov, and O. Buchnev, "Ferroelectric particles in liquid crystals: Recent frontiers," *Molecular Crystals and Liquid Crystals*, vol. 453, pp. 227-237, 2006, doi: 10.1080/15421400600653852.

[21] V. Y. Reshetnyak, S. M. Shelestiuk, and T. J. Sluckin, "Freedericksz transition threshold in nematic liquid crystals filled with ferroelectric nanoparticles," *Molecular Crystals and Liquid Crystals*, vol. 454, pp. 201-206, 2006, doi: 10.1080/15421400600654108.

[22] F. Li, J. West, A. Glushchenko, C. Cheon, and Y. Reznikov, "Ferroelectric nanoparticle/liquid-

crystal colloids for display applications," *Journal of the Society for Information Display*, vol. 14, pp. 523-527, 2006, doi: 10.1889/1.2210802.

[23] S. Kaur, S. P. Singh, A. M. Biradar, A. Choudhary, and K. Sreenivas, "Enhanced electro-optical properties in gold nanoparticles doped ferroelectric liquid crystals," *Applied Physics Letters*, vol. 91, 023120, 2007, doi: 10.1063/1.2756136.

[24] O. Buchnev, A. Dyadyusha, M. Kaczmarek, V. Reshetnyak, and Y. Reznikov, "Enhanced two-beam coupling in colloids of ferroelectric nanoparticles in liquid crystals," *Journal of the Optical Society of America B*, vol. 24, pp. 1512-1516, 2007, doi: 10.1364/JOSAB.24.001512.

[25] M. Copic, A. Mertelj, O. Buchnev, and Y. Reznikov, "Coupled director and polarization fluctuations in suspensions of ferroelectric nanoparticles in nematic liquid crystals," *Physical Review E*, vol. 76, 011702, 2007, doi: 10.1103/PhysRevE.76.011702.

[26] G. Cook, A. V. Glushchenko, V. Reshetnyak, A. T. Griffith, M. A. Saleh, and D. R. Evans, "Nanoparticle doped organic-inorganic hybrid photorefractives," *Optics Express*, vol. 16, pp. 4015-4022, 2008, doi: 10.1364/OE.16.004015.

[27] M. Kaczmarek, O. Buchnev, and I. Nandhakumar, "Ferroelectric nanoparticles in low refractive index liquid crystals for strong electro-optic response," *Applied Physics Letters*, vol. 92, 103307, 2008, doi: 10.1063/1.2884186.

[28] J. Prakash, A. Choudhary, A. Kumar, D. S. Mehta, and A. M. Biradar, "Nonvolatile memory effect based on gold nanoparticles doped ferroelectric liquid crystal," *Applied Physics Letters*, vol. 93, 112904, 2008, doi: 10.1063/1.2980037.

[29] A. Kumar, J. Prakash, D. S. Mehta, A. M. Biradar, and W. Haase, "Enhanced photoluminescence in gold nanoparticles doped ferroelectric liquid crystals," *Applied Physics Letters*, vol. 95, 023117, 2009, doi: 10.1063/1.3179577.

[30] M. S. S. Pereira, A. A. Canabarro, I. N. de Oliveira, M. L. Lyra, and L. V. Mirantsev, "A

molecular dynamics study of ferroelectric nanoparticles immersed in a nematic liquid crystal," *European Physical Journal E*, vol. 31, pp. 81-87, 2010, doi: 10.1140/epje/i2010-10553-y.

[31] J.-F. Blach, S. Saitzek, C. Legrand, L. Dupont, J.-F. Henninot, and M. Warengem, "BaTiO₃ ferroelectric nanoparticles dispersed in 5CB nematic liquid crystal: Synthesis and electro-optical characterization," *Journal of Applied Physics*, vol. 107, 074102, 2010, doi: 10.1063/1.3369544.

[32] M. Gupta, I. Satpathy, A. Roy, and R. Pratibha, "Nanoparticle induced director distortion and disorder in liquid crystal-nanoparticle dispersions," *Journal of Colloid and Interface Science*, vol. 352, pp. 292-298, 2010, doi: 10.1016/j.jcis.2010.08.027.

[33] H.-H. Liang, Y.-Z. Xiao, F.-J. Hsu, C.-C. Wu, and J.-Y. Lee, "Enhancing the electro-optical properties of ferroelectric liquid crystals by doping ferroelectric nanoparticles," *Liquid Crystals*, vol. 37, pp. 255-261, 2010, doi: 10.1080/02678290903564403.

[34] M. R. Herrington, O. Buchnev, M. Kaczmarek, and I. Nandhakumar, "The effect of the size of BaTiO₃ nanoparticles on the electro-optic properties of nematic liquid crystals," *Molecular Crystals and Liquid Crystals*, vol. 527, pp. 72-79, 2010, doi: 10.1080/15421406.2010.486362.

[35] G. Cook, V. Y. Reshetnyak, R. F. Ziolo, S. A. Basun, P. P. Banerjee, and D. R. Evans, "Asymmetric Fredericksz transitions from symmetric liquid crystal cells doped with harvested ferroelectric nanoparticles," *Optics Express*, vol. 18, pp. 17339-17345, 2010, doi: 10.1364/OE.18.017339.

[36] S. A. Basun, G. Cook, V. Y. Reshetnyak, A. V. Glushchenko, and D. R. Evans, "Dipole moment and spontaneous polarization of ferroelectric nanoparticles in a nonpolar fluid suspension," *Physical Review B*, vol. 84, 024105, 2011, doi: 10.1103/PhysRevB.84.024105.

[37] S. M. Shelestiuk, V. Y. Reshetnyak, and T. J. Sluckin, "Frederiks transition in ferroelectric liquid-crystal nanosuspensions," *Physical Review E*, vol. 83, 041705, 2011, doi: 10.1103/PhysRevE.83.041705.

- [38] L. M. Lopatina and J. V. Selinger, "Maier-Saupe-type theory of ferroelectric nanoparticles in nematic liquid crystals," *Physical Review E*, vol. 84, 041703, 2011, doi: 10.1103/PhysRevE.84.041703.
- [39] S. Ghosh, S. K. Roy, S. Acharya, P. K. Chakrabarti, M. Zurowska, and R. Dabrowski, "Effect of multiferroic BiFeO₃ nanoparticles on electro-optical and dielectric properties of a partially fluorinated orthoconic antiferroelectric liquid crystal mixture," *EPL*, vol. 96, 47003, 2011, doi: 10.1209/0295-5075/96/47003.
- [40] L. Wang et al., "Low voltage and hysteresis-free blue phase liquid crystal dispersed by ferroelectric nanoparticles," *Journal of Materials Chemistry*, vol. 22, pp. 19629-19633, 2012, doi: 10.1039/c2jm34013e.
- [41] P. Malik, A. Chaudhary, R. Mehra, and K. K. Raina, "Electrooptic and dielectric studies in cadmium sulphide nanorods/ferroelectric liquid crystal mixtures," *Advances in Condensed Matter Physics*, vol. 2012, Art. no. 853160, 2012, doi: 10.1155/2012/853160.
- [42] A. Ghandevosyan and R. Hakobyan, "Decrease in the threshold of electric Fredericksz transition in nematic liquid crystals doped with ferroelectric nanoparticles," *Journal of Contemporary Physics*, vol. 47, pp. 33-35, 2012, doi: 10.3103/S1068337212010070.
- [43] A. Mertelj, L. Cmok, M. Copic, G. Cook, and D. R. Evans, "Critical behavior of director fluctuations in suspensions of ferroelectric nanoparticles in liquid crystals at the nematic to smectic-A phase transition," *Physical Review E*, vol. 85, 021705, 2012, doi: 10.1103/PhysRevE.85.021705.
- [44] A. Lapanik, D. Wojnowska, and W. Haase, "Influence of chain length and tethered liquid crystal groups of functionalized gold nanoparticles on thermotropic, dielectric and electro-optical properties of ferroelectric liquid crystal nanocolloids," *Soft Matter*, vol. 8, pp. 10195-10207, 2012, doi: 10.1039/C2SM25991E.
- [45] A. Rudzki, D. R. Evans, G. Cook, and W. Haase, "Size dependence of harvested BaTiO₃ nanoparticles on the electro-optic and dielectric properties of ferroelectric liquid crystal nanocolloids," *Applied Optics*, vol. 52, pp. E6-E14, 2013, doi: 10.1364/AO.52.0000E6.
- [46] R. Basu and A. Garvey, "Effects of ferroelectric nanoparticles on ion transport in a liquid crystal," *Applied Physics Letters*, vol. 105, 151905, 2014, doi: 10.1063/1.4898581.
- [47] U. B. Singh, S. Dhar, N. S. Pandey, V. K. Misra, and H. S. Pandey, "Enhanced electro-optical properties of a nematic liquid crystal dispersed with gold nanoparticles," *Liquid Crystals*, vol. 41, pp. 953-959, 2014, doi: 10.1080/02678292.2014.894209.
- [48] Y. Garbovskiy and I. Glushchenko, "Ion trapping by means of ferroelectric nanoparticles, and the quantification of this process in liquid crystals," *Applied Physics Letters*, vol. 107, 041106, 2015, doi: 10.1063/1.4926988.
- [49] M. V. Rasna, L. Cmok, D. R. Evans, A. Mertelj, and S. Dhara, "Phase transitions, optical, dielectric and viscoelastic properties of colloidal suspensions of BaTiO₃ nanoparticles and cyanobiphenyl liquid crystals," *Liquid Crystals*, vol. 42, pp. 1059-1067, 2015, doi: 10.1080/02678292.2015.1021719.
- [50] C. Cirtoaje, E. Petrescu, and V. Stoian, "Electrical Fredericksz transitions in nematic liquid crystals containing ferroelectric nanoparticles," *Physica E*, vol. 67, pp. 23-27, 2015, doi: 10.1016/j.physe.2014.11.004.
- [51] F. V. Podgornov, R. Wipf, B. Stuhn, A. V. Ryzhkova, and W. Haase, "Low-frequency relaxation modes in ferroelectric liquid crystal/gold nanoparticle dispersion: Impact of nanoparticle shape," *Liquid Crystals*, vol. 43, pp. 1536-1547, 2016, doi: 10.1080/02678292.2016.1186754.
- [52] P. Kumar, A. Kishore, and A. Sinha, "Analog switching in the nanocolloids of ferroelectric liquid crystals," *Applied Physics Letters*, vol. 108, 262903, 2016, doi: 10.1063/1.4955023.
- [53] R. K. Shukla, D. R. Evans, and W. Haase, "Ferroelectric BaTiO₃ and LiNbO₃ nanoparticles dispersed in ferroelectric liquid crystal mixtures: Electrooptic and dielectric parameters influenced by

properties of the host, the dopant and the measuring cell," *Ferroelectrics*, vol. 500, pp. 141-152, 2016, doi: 10.1080/00150193.2016.1215206.

[54] F. V. Podgornov, M. Gavriyak, A. R. Karaawi, V. Boronin, and W. Haase, "Mechanism of electrooptic switching time enhancement in ferroelectric liquid crystal/gold nanoparticles dispersion," *Liquid Crystals*, vol. 45, pp. 1594-1602, 2018, doi: 10.1080/02678292.2018.1458256.

[55] A. R. Karaawi, M. V. Gavriyak, V. A. Boronin, A. M. Gavriyak, J. V. Kazachonok, and F. V. Podgornov, "Direct current electric conductivity of ferroelectric liquid crystals-gold nanoparticles dispersion measured with capacitive current technique," *Liquid Crystals*, vol. 47, pp. 1507-1515, 2020, doi: 10.1080/02678292.2020.1740951.